Nonlinear Low-Force Elasticity of Single-Stranded DNA Molecules

O. A. Saleh,[1,*] D. B. McIntosh,[2] P. Pincus,[1,2] and N. Ribeck[2]

[1]*Materials Department and BMSE Program, University of California, Santa Barbara, California 93106, USA*
[2]*Physics Department, University of California, Santa Barbara, California 93106, USA*

(Received 12 August 2008; published 11 February 2009)

We reconcile single-molecule force-extension data with scaling theories of polymer elasticity: measurements of denatured single-stranded DNA show a regime where the extension grows as a nonlinear power law with force, in accordance with "tensile blob" models. Analysis of the salt dependence of this regime indicates that the polymer's Kuhn length is proportional to the Debye length; this contradicts the Odijk-Skolnick-Fixman theory, but agrees with other predictions. Finally, we identify a Θ condition of the polymer, and find that the wormlike chain model best describes the polymer's elasticity at this point.

DOI: 10.1103/PhysRevLett.102.068301 PACS numbers: 82.37.Rs, 82.35.Rs, 87.15.La

The structural properties of a single polymer are well described by scaling theories that account both for the polymer's local bending stiffness and for interactions between monomers well separated on the chain (i.e., "excluded-volume" interactions) [1,2]. For polymers in a good solvent, scaling theory predicts a self-avoiding random-walk structure whose properties are in quantitative agreement with scattering measurements of dilute polymer solutions [2]. More recently, single-molecule manipulation experiments have emerged as alternative probes of polymer conformation and have led to significant progress in understanding the fundamental properties of a variety of polymers, notably single- and double-stranded nucleic acids [3–6]. Single-molecule experiments measure the end-to-end extension of a single polymer that is stretched with a known force. The resulting extension versus force data are typically compared to models that attribute the polymer's local stiffness either to the bending of discrete, flexible joints between rigid Kuhn segments of length l [the "freely jointed chain" (FJC) [2]] or to the continuous bending elasticity of a thin rod [the "wormlike chain" (WLC) [4]]. While the FJC and WLC models account for local stiffness, they ignore long-range monomer interactions. Thus, they are ideal models that differ fundamentally from the established scaling picture of real polymers.

The FJC and WLC models are successful in describing manipulation experiments because the applied force effectively screens long-range interactions: the applied force f creates a tensile screening length $\xi \sim T/f$, where T is the thermal energy. For monomers separated by more than ξ, the force dominates thermal fluctuations, preventing their interaction. Most experiments have been performed in the regime $\xi < l$ (either because the apparatus is limited to applying high forces or because l is large, as in the case of double-stranded DNA), so all monomer interactions are cut off, and ideal models are applicable. A notable exception is experiments on single-stranded nucleic acids that have accessed the $\xi \gtrsim l$ regime and observed effects of long-range interactions [5–7]. However, no definitive connection has yet been made between single-molecule force-extension data and analytical theories of nonideal chains.

Here, we perform force-extension measurements on chemically denatured single-stranded DNA (d-ssDNA) over a wide range of salt concentrations c and demonstrate a quantitative link between our data and scaling models of nonideal polymers under tension. Our major results are as follows. (i) For over two decades in c, and at low forces, we observe the measured extension L to increase as a nonlinear power law with f: $L \sim f^{\gamma}$, with $\gamma \approx 0.60$–0.69. This is consistent with the "tensile blob" scaling model, which predicts $\gamma = 2/3$ [8]; to our knowledge, this is the first experimental confirmation of that prediction. (ii) By analyzing the salt dependence of the power-law regime, we extract the dependence of l and the effective excluded-volume parameter v on c. In particular, we find that $l \sim c^{-\delta}$ with $\delta \approx 0.4$–0.5. The dependence of l on c has been a subject of extensive theoretical discussion [9]: the well-known Odijk-Skolnick-Fixman (OSF) [10,11] theory gives $\delta = 1$, while other theories [9] predict $\delta = 0.5$. Our data provide strong support for the latter results. (iii) We identify $c \approx 3\ M$ as a Θ point of the polymer, where $v = 0$ and the polymer acts ideally. At the Θ point, the data are best fit by a WLC model [4], rather than a FJC model. From the fits, we extract a "bare" (nonelectrostatic) persistence length of ≈ 0.6 nm for d-ssDNA.

Scaling theory.—To model the behavior of a real polymer under tension, we first consider its tension-free structure (throughout, we utilize a scaling approach that ignores numerical prefactors). We model the polymer as a chain of N statistical monomers each having a Kuhn length l, where the contour length $L_0 \equiv Nl$. In the Flory approximation [1], the rms size of the chain R_0 is

$$R_0 \sim L_0^{3/5}\left(\frac{v}{l}\right)^{1/5}, \tag{1}$$

where the excluded-volume parameter v includes all interactions between Kuhn segments.

 © 2009 The American Physical Society

The Flory picture can be applied to derive the dependence of the stretched end-to-end length L on f using a scaling argument [8]: Since R_0 is the characteristic length of the polymer, L will scale with R_0. In particular, $L \sim R_0\Psi(R_0/\xi)$, where the form of the function $\Psi(x)$ varies with ξ. For $\xi > R_0$, the length should respond linearly with force; this occurs if $\Psi(x) \sim x$, giving $L \sim R_0^2 f/T$. As the force is increased into the intermediate regime, $\xi < R_0$, the polymer becomes strongly stretched: $L \sim L_0$. To satisfy this constraint with a power-law function, and given Eq. (1), requires $\Psi(x) \sim x^{2/3}$ so that

$$L \sim L_0\left(\frac{v}{l}\right)^{1/3}\left(\frac{f}{T}\right)^{2/3}. \tag{2}$$

Equation (2) depends on the Flory relation [Eq. (1)]; thus, it holds only when significant monomer interactions are present. In the intermediate regime, these interactions occur within subsections of the polymer ("blobs") that adopt a self-avoiding random-walk structure on length scales less than ξ.

As the force increases, ξ decreases until the blobs contain too few monomers to be viewed as swollen polymers, and Eq. (2) will no longer apply. Most simply, this can be predicted to occur at a crossover point $\xi_c \sim l$ (i.e., when each blob contains a single Kuhn segment), so that the high-force end point (f_c, L_c) of the intermediate regime will occur at

$$f_c \sim T/l, \qquad L_c/L_0 \sim (v/l^3)^{1/3}. \tag{3}$$

Alternatively, the end point could occur when the excluded-volume interaction energy per blob decreases to T. Then the interactions become negligible, and the subsections behave as ideal chains ("thermal blobs") of size $b \sim l^4/v$ [2]. In this case, the end point occurs at $\xi_c \sim b$, so that

$$f_c \sim Tv/l^4, \qquad L_c/L_0 \sim v/l^3. \tag{4}$$

Since we independently measure f_c and L_c/L_0, we can estimate v and l from Eqs. (3) and (4) without assuming a relation between v and l.

Experiments.—Single-stranded nucleic acids (ssNAs) are polyelectrolytes with Kuhn lengths short enough to allow experimental access to force regimes $\xi \gtrsim l$ [5,6]. Using ssNAs as model systems is complicated by the possibility of intrastrand base pairing. Here, following the approach of Dessinges *et al.* [5], we utilize ssDNA to test force-extension behavior, and methods of chemical denaturation to avoid base pairing. Labeled ssDNAs are generated by polymerase chain reaction amplification of a 10.5 kilo-base pair segment of the Lambda phage genome using 5'-labeled primers, 3' labeling using terminal transferase, and thermal denaturation. Permanent chemical denaturation is then achieved using reaction with glyoxal [12]. Some d-ssDNA made in this fashion are shorter than expected; we attribute this to the presence of glyoxal cross-links [13] that sequester a loop of ssDNA. Controls using formaldehyde as the denaturant show the expected lengths, and, when scaled by L_0, an identical relative variation of extension with force as glyoxal-denatured ssDNA. Thus, we conclude that the apparent cross-linking does not affect polymer elasticity, and utilize glyoxal in the experiments presented here. Force-extension measurements are performed in a magnetic tweezer in which the labels are used to tether d-ssDNA between a magnetic bead and a glass surface; force and extension are measured as described [14]. Experiments were performed in a sodium phosphate buffer, pH ≈ 6.5; NaCl was added to the buffer to obtain the desired monovalent salt concentration c.

For c between 20 mM and 2 M, all force-extension curves show two behaviors demarcated by a crossover force, f_c (Fig. 1): for $f < f_c$, L increases with f as a nonlinear power law, while for $f > f_c$, L increases as $\ln(f)$. The value of f_c increases with c; for $c < 20$ mM, the power-law regime presumably occurs, but at forces too low to measure. At no value of c do we observe a low-force transition from a nonlinear power law to a linear behavior; we thus conclude that the linear-response regime is inaccessible in this experiment.

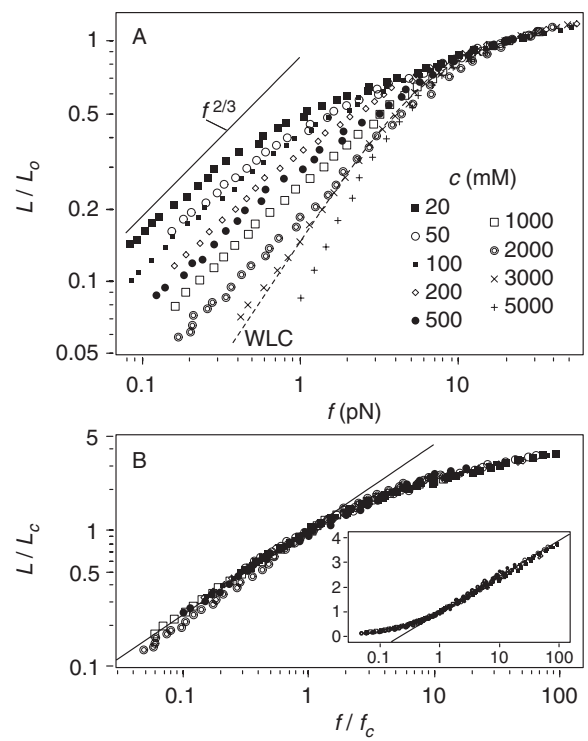

FIG. 1. (a) Representative data of relative length [scaled by $L_0 \approx L(f = 20\text{ pN})$; see text] versus force for d-ssDNA at various salt concentrations. The solid line indicates the slope of the predicted power law, and the dashed line is the best-fit WLC model to the 3 M data with $l_p = 0.65$ nm. (b) Data from (a) between 20 mM and 2 M replotted with L and f scaled by the crossover values L_c and f_c. The line is the power law $L \sim f^{0.63}$. Inset: The same data, plotted on lin-log axes to emphasize the high-force logarithmic behavior; the line indicates $L \sim 0.63\ln(f)$.

We fit the low-force points to a power law, $L \sim f^{\gamma}$, and extract the dependence of γ on c (Fig. 2). For c between 20 mM and 2 M, the exponent is relatively stable, rising slightly from $\gamma \approx 0.60$ to ≈ 0.69, while for $c > 2\ M$, γ strongly increases with salt. The value of γ below 2 M is consistent with Eq. (2); thus, we conclude that our low-force data corresponds to the intermediate-force regime of the scaling analysis. For $c < 1\ M$, the measured value of γ is lower than the prediction; such a deviation agrees with recent simulations [15] and is due to a slight stretching within the tensile blobs by the applied force. This effect becomes negligible as the number of statistical monomers N in the chain increases [15]: since N increases with c (due to the decrease of l with c; see below), the measured exponent more closely matches the prediction at $c = 1.5$ and 2 M.

A logarithmic regime has been observed previously [5,6]. It coincides with an extensible FJC (EFJC) model only for very high forces [5]; agreement over a wider (though not complete) force range can be found by implementing a scale-dependent persistence length [6]. A logarithmic regime is consistent with our scaling model: In the intermediate regime [Eq. (2)], the polymer is already strongly stretched, $L \sim L_0$. Thus, when that regime breaks down ($f > f_c$), there cannot be a stronger-stretching regime with a new power-law behavior of $\Psi(x)$. Instead, the behavior must be sub-power-law, which most easily occurs if $\Psi(x) \sim \ln(x)$, giving $L \sim \ln(f)$. In practice, this relation can be made more precise by forcing it to be both continuous and smooth with the power-law regime at the crossover point (f_c, L_c). In particular, the data between 20 mM and 2 M are well described by

$$L = L_c(f/f_c)^{\gamma} H(f_c - f) + L_c[\gamma \ln(f/f_c) + 1] H(f - f_c), \tag{5}$$

where $H(x) = 0$ (1) for $x < 0$ (≥ 0). We fixed γ to the value found from power-law fits at each c, and fit Eq. (5) to each curve using only two free parameters, f_c and L_c. The success of Eq. (5) is demonstrated by the collapse of the force-extension data at 20 m$M \leq c \leq 2\ M$ when scaled by the fit values of f_c and L_c [Fig. 1(b)].

Applying Eqs. (3) and (4) requires an estimate of L_0. We extract a model-independent estimate by interpolating each L versus f curve at 20 pN, and setting $L_0 = L(f = 20\text{ pN})$. We choose 20 pN because, for $f > 20$ pN, the salt-dependent effects on $L(f)$ disappear [Fig. 1(a)]. We also made alternate estimates of L_0 using fits of various regimes of the high-force data ($f > 10$, 20 or 30 pN) to both EFJC and WLC models. While the absolute value of L_0 varies with the method used, the value from a particular method deviates from $L(20\text{ pN})$ by a multiplicative factor that is constant for all c. Since our analysis ignores prefactors, the absolute variation is unimportant, and we use $L_0 = L(20\text{ pN})$ throughout.

In the range 20 m$M \leq c \leq 2\ M$, we find both f_c and the ratio L_c/L_0 increase monotonically with c (Fig. 3); power-law fits give $f_c \sim c^{0.54\pm0.03}$ and $L_c/L_0 \sim c^{0.11\pm0.01}$. From the f_c and L_c/L_0 values, we can extract estimates of l and υ using Eq. (3) or Eq. (4). These equations assume $\gamma = 2/3$, which differs slightly from the measured value. However, we have found only a $\approx 10\%$ difference in the results depending on which exponent is used; thus, we ignore the difference, and include the 10% in the estimated uncertainty. We find that l and υ decrease with c, with the best-fit power-law exponent varying slightly between the models: Using Eq. (3), we find $l \sim c^{-0.51\pm0.04}$ (note that this value is not dependent on γ) and $\upsilon \sim c^{-1.09\pm0.17}$. Alternatively, using Eq. (4), we find $l \sim c^{-0.40\pm0.04}$ and $\upsilon \sim c^{-0.97\pm0.17}$.

The dependence of l on the Debye length $\lambda_D \sim c^{-0.5}$ has been studied in a variety of ways [9], most famously in the OSF theory [10,11]. In the OSF approach, the total Kuhn length is $l = l_e + l_0$, where l_e (l_0) is the electrostatic (structural) contribution to the polymer's stiffness. By estimating the electrostatic energy of a bent polymer, OSF predicts $l_e \sim \lambda_D^2$, which is inconsistent with our result. However, the OSF theory does match data from micromanipulation measurements of double-stranded

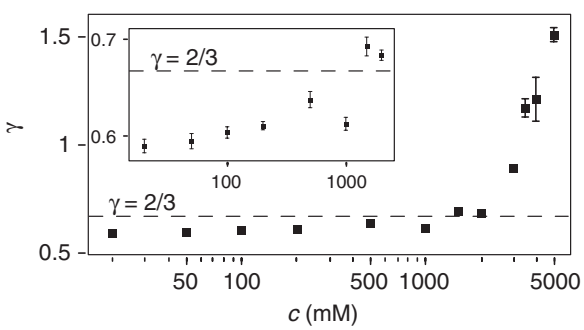

FIG. 2. Measured power-law exponent γ versus salt concentration c from 69 force-extension curves, with between 2 and 10 curves averaged per point. Inset: Detail of the regime 20 m$M \leq c \leq 2\ M$.

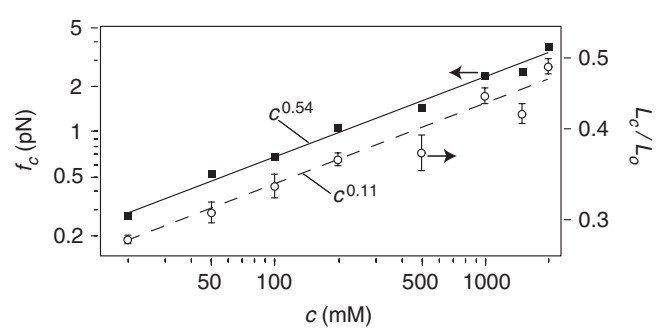

FIG. 3. The crossover force f_c (filled squares) and the relative crossover length L_c/L_0 (open circles) versus salt concentration c. The data are from 54 force-extension curves, with between 2 and 10 curves averaged per point. The continuous (dashed) line is the best-fit power law to the f_c (L_c/L_0) data, with exponent as shown.

DNA (dsDNA) [16]. Those measurements differ from ours in several ways: dsDNA is a torsionally constrained, highly stiff ($l_0 \approx 90$ nm) polymer, and the dsDNA experiments were performed in the regime $\lambda_D \ll l_0$ and $\xi \ll l$. In contrast, ssDNA is a torsionally free, flexible ($l_0 \approx 1.2$ nm; see below) polymer, and our results are found for both $\lambda_D \gtrsim l_0$ and $\lambda_D \lesssim l_0$, and for $\xi \gtrsim l$. The different experimental results are likely due to these physical differences. At least two extensions of the OSF theory might reconcile the results: Barrat and Joanny [17] introduce configurational fluctuations, and predict $l_e \sim \lambda_D$ for highly flexible polymers, and $l_e \sim \lambda_D^2$ for stiff polymers, consistent with both experiments. More recently, Dobrynin [18] noted that OSF theory ignores the polymer's torsional degrees of freedom, which implies OSF would apply to dsDNA but not ssDNA. Adding torsional freedom to the OSF approach gives $l_e \sim \lambda_D$ [18], which is consistent with our results.

The exponent γ increases for $c > 2\ M$, reaching $\gamma \approx 1$ at $c \approx 3\ M$ (Fig. 2). Since a broad linear regime is expected for an ideal polymer, we interpret $c \approx 3\ M$ as a Θ point of d-ssDNA: the screened electrostatic repulsion between monomers is equal in magnitude to the weak attractive forces (e.g., van der Waals or hydrophobic interactions), and $\upsilon = 0$. If this is true, then the increased screening at $c > 3\ M$ should lead to monomer aggregation. Indeed, we observe evidence of this: we find $\gamma > 1$ for $c > 3\ M$ (Fig. 2), indicating the presence of aggregates that break apart under applied force, causing L to increase rapidly with f. Values of $\gamma > 1$ are consistent with scaling predictions: In a poor solvent, the polymer size scales as $R_0 \sim N^{1/3}$. Using this, and following the argument that led to Eq. (2), gives $\gamma = 2$. The measured values reach $\gamma \approx 1.5$ at the limit set by the solubility of the salt, and are still increasing at that point; thus our data are not inconsistent with the prediction.

We exploit the ideal behavior at the Θ point to evaluate ideal models of polymer elasticity. We fit the force-extension data at $c = 3\ M$ using both the EFJC model [7] with three free parameters (L_0, l, and stretch modulus K) and the WLC model [4] with two free parameters (L_0 and the persistence length $l_p = l/2$) [19]. The χ^2 for the WLC fits is $\approx 15\%$ better than the EFJC fits. Further, the EFJC fits produce values of $K \approx 200$ pN, anomalously low compared to the values found in higher-force experiments [7,20]. We conclude that the WLC model provides a better description of the elasticity of d-ssDNA in Θ conditions. The fit value $l_{p,\Theta}$ is indicative of d-ssDNA's "bare" structural stiffness: averaged over three curves, we find $l_{p,\Theta} = 0.62 \pm 0.01$ nm, and thus a bare Kuhn length $l_0 = 1.24 \pm 0.02$ nm.

Our work demonstrates a direct link between single-molecule force-extension data and scaling models of polymer elasticity. We find a regime of nonlinear elasticity predicted by scaling, but not previously observed. Analysis of the salt dependence of that regime indicates that the polymer's Kuhn length is proportional to the Debye length. Finally, we determine a Θ point for d-ssDNA and use it both to evaluate ideal models of elasticity and to extract the structural persistence length. Future work is needed to understand the nature of the logarithmic regime, to confirm the source of the measured deviation of γ from $2/3$, to find the linear-response regime, and to test the effects of multivalent salts, for which the Debye-Huckel assumptions that underlie the predictions of l versus c break down.

This work was supported by the NSF under Grants No. PHY-0748564, No. DMR-0503347, No. DMR-0710521, and No. DMR-0520415. We thank D. Thirumalai and A. V. Dobrynin for helpful conversations.

*saleh@engineering.ucsb.edu

[1] P. G. de Gennes, *Scaling Concepts in Polymer Physics* (Cornell University, Ithaca, NY, 1979).
[2] M. Rubinstein and R. H. Colby, *Polymer Physics* (Oxford University, New York, 2003).
[3] C. Bustamante, J. F. Marko, E. D. Siggia, and S. Smith, Science **265**, 1599 (1994).
[4] J. F. Marko and E. D. Siggia, Macromolecules **28**, 8759 (1995).
[5] M. N. Dessinges, B. Maier, Y. Zhang, M. Peliti, D. Bensimon, and V. Croquette, Phys. Rev. Lett. **89**, 248102 (2002).
[6] Y. Seol, G. M. Skinner, and K. Visscher, Phys. Rev. Lett. **93**, 118102 (2004).
[7] S. B. Smith, Y. J. Cui, and C. Bustamante, Science **271**, 795 (1996).
[8] P. Pincus, Macromolecules **9**, 386 (1976).
[9] A. V. Dobrynin and M. Rubinstein, Prog. Polym. Sci. **30**, 1049 (2005), and references therein.
[10] T. Odijk, J. Polym. Sci. B **15**, 477 (1977).
[11] J. Skolnick and M. Fixman, Macromolecules **10**, 944 (1977).
[12] G. K. McMaster and G. G. Carmichael, Proc. Natl. Acad. Sci. U.S.A. **74**, 4835 (1977).
[13] H. Kasai, N. Iwamoto-Tanaka, and S. Fukada, Carcinogenesis **19**, 1459 (1998).
[14] N. Ribeck and O. A. Saleh, Rev. Sci. Instrum. **79**, 094301 (2008), and references therein.
[15] G. Morrison, C. Hyeon, N. M. Toan, B. Y. Ha, and D. Thirumalai, Macromolecules **40**, 7343 (2007).
[16] C. G. Baumann, S. B. Smith, V. A. Bloomfield, and C. Bustamante, Proc. Natl. Acad. Sci. U.S.A. **94**, 6185 (1997).
[17] J. L. Barrat and J. F. Joanny, Europhys. Lett. **24**, 333 (1993).
[18] A. V. Dobrynin, Macromolecules **38**, 9304 (2005).
[19] Nonextensible FJC models fail to adequately fit the data, and extensible WLC models do not significantly improve over the WLC fits; thus, we do not discuss them in detail.
[20] M. Rief, H. Clausen-Schaumann, and H. E. Gaub, Nat. Struct. Mol. Biol. **6**, 346 (1999).